ORIGINAL RESEARCH ARTICLE

Preparation and decarburization characteristics of SiO_2-Al_2O_3 composite aerogel modified by potassium carbonate

Jingnan Guo, Yanlin Wang, Baihe Guo, Xiaolei Qiao, Xiaofei Wang, Jinrong Guo, Yan Jin[*]

School of Electrical and Power Engineering, Taiyuan University of Technology, Taiyuan 030024, China. E-mail: jinyan@tyut.edu.cn

ABSTRACT

In this paper, the preparation of potassium carbonate modified SiO_2-Al_2O_3 composite aerogel, the carbonation characteristics of K_2CO_3 and the decarburization characteristics of regeneration cycle were studied. The influence of loading rate on CO_2 adsorption was studied by using a fixed bed reactor, and the microstructure of the samples was analyzed by combining SEM and BET. The results show that during the alkali fusion sintering of Na_2CO_3, the Si-O-Si and Si-O-Al bonds break, the crystal structure is destroyed, and the covalent bond of mullite is transformed into the ionic bond of nepheline. Through orthogonal test, taking the specific surface area of aerogel as the measurement index, the optimal calcination conditions are determined as follows: 900 °C, reaction for 60 min, Na_2CO_3 addition ratio of 0.5. The more K_2CO_3 is loaded, the less the corresponding active sites on the surface of the carrier. When the loading is 30%, the maximum CO_2 adsorption capacity is 2.86 mmol·g^{-1}. Excess K_2CO_3 will plug the pore structure, destroy the diffusion of CO_2, and reduce the diffusion and utilization efficiency. The percentage of mesoporous pore volume decreased from 94.21% to 89.32%, indicating that the active component K_2CO_3 was mainly filled in the mesoporous. After 10 cycle regeneration tests, the CO_2 adsorption capacity of the adsorbent decreased by 10.49%. The pore structure of the adsorbent was stable and the decarburization performance was excellent.

Keywords: SiO_2-Al_2O_3 Composite Aerogel; CO_2 Adsorption; Carbonation Characteristics; Microscopic Characteristics

ARTICLE INFO

COPYRIGHT

1. Introduction

Climate problem has become a global problem. According to the relevant data analysis of CAIT (World Resources Institute), the world's CO_2 emissions have increased at an annual growth rate of 2.4% in the past decade[1]. China's carbon emissions rank first in the world, and the implementation of low-carbon development strategy is of great practical significance to slow down global warming[2].

Alkali metal based solid adsorbent technology for low-temperature removal of CO_2 from flue gas has low reaction temperature, fast reaction rate between adsorbent and CO_2, high conversion rate and no secondary pollution[3]. The research on new carbon dioxide adsorbents with amino groups as active components and porous materials is relatively mature. Among them, the adsorption capacity of amino modified mesoporous silica aerogel gel adsorbent (AMSA) can reach 6.97 mmol·g^{-1} at 25 °C[4]. Sodium based adsorbents are rich in resources and low in price, but their reactivity is low[5]. After carbonation, the internal structure of calcium based adsorbent sintered, resulting in a sharp decline in the adsorption rate, and SO_2 in the waste gas reacted with CaO to produce $CaSO_4$, which could not be regenerated, reducing the effective content of CaO and the adsorption performance[6].

CO_2 adsorbent with potassium as the active component is a research hotspot in recent years. According to different carrier materials, domestic and foreign scholars have carried out a series of decarburization characteristics, as shown in **Table 1**. Research shows that potassium carbonate is combined with carrier materials with developed microstructure and high mechanical strength to improve the utilization rate of potassium carbonate and greatly improve the carbonation performance[7].

Table 1. Comparison of CO_2 adsorption capacity of K_2CO_3-based adsorbent

Adsorbent	K_2CO_3 load/%wt	Adsorption conditions	Conversion rates/%	CO_2 adsorption capacity/mmol·g^{-1}	References
K_2CO_3/AC	30	60°C, 1%CO_2 + 9%H_2O	—	1.95	[8,9]
	30	20°C, 0.5%CO_2 + 1.8%H_2O	—	0.87	[10]
K_2CO_3/AC1	30	60°C, 15%CO_2 + 15%H_2O	89.20	—	[11]
K_2CO_3/AC2	30	60°C，15% CO_2 + 15%H_2O	87.90	—	[11]
K_2CO_3/Al_2O_3	30	60°C, 1%CO_2 + 9%H_2O	—	1.93	[8,9]
	24.5	60°C, 18%CO_2 + 18%H_2O	95.20	—	[12]
	30	20°C, 0.5%CO_2 + 1.8%H_2O	—	1.18	[10]
K_2CO_3/MgO	30	60°C, 1%CO_2 + 9%H_2O	—	2.70	[8,9]
K_2CO_3/5A	33	70°C, 5%CO_2 + 10%H_2O	78.20	—	[13]
	30	20°C, 0.5% CO_2 + 1.8%H_2O	—	0.34	[10]
K_2CO_3/SG	20	20°C, 1%CO_2 + 2%H_2O	88.62	1.32	[14]
	30	60°C, 15%CO_2 + 15%H_2O	18.80	—	[11]
K_2CO_3/SiO_2	30	60°C, 1%CO_2 + 9%H_2O	—	0.23	[8,9]
K_2CO_3/ZrO_2	30	60°C, 1%CO_2 + 9%–11%H_2O	—	1.73–1.87	[6,15]
K_2CO_3/DT	19.1	60°C, 18%CO_2 + 18%H_2O	33.90	—	[12]
K_2CO_3/TiO_2	30	60°C, 1%CO_2 + 9%H_2O	—	1.89–2.05	[8,9]

Due to the influence of the micro characteristics of the carrier itself, the loading capacity of K_2CO_3 is limited, so that the microstructure and adsorption capacity of the adsorbent are limited due to saturated loading. Therefore, it is necessary to prepare a carrier material with good micro characteristics and load the active component K_2CO_3 to make a modified potassium-based adsorbent with high CO_2 adsorption capacity and low cost. Aerogel gel is an amorphous nano porous material with high specific surface area, high porosity and low density. It is widely used in the fields of adsorption, catalysis and catalyst support. Yu et al.[17] prepared alumina aerogel with aluminium tri-sec-butoxide as precursor, with high thermal stability and specific surface area of 744.50 m²·g^{-1}. Guo et al. used TEOS as silicon source to prepare silicon gel, loaded with K_2CO_3 as adsorbent, the CO_2 adsorption capacity can reach 1.32 mmol·g^{-1}, and the carbonation performance is excellent[14]. Silicon and aluminum sources using TEOS and organic alkoxides as sols are not only costly but also toxic[16] and the above research is limited to ultra-low CO_2 concentration, which cannot meet the flue gas atmosphere of coal-fired power plants.

The fly ash discharged from dust collectors of coal-fired power plants is one of the largest industrial wastes in the world at present, and its main chemical components are SiO_2 and Al_2O_3. Liu et al.[18] prepared binary composite aerogel from coal gangue, with a specific surface area of 483.23 m²·g^{-1} and a specific pore volume of 1.87 cm³·g^{-1}; Chen et al.[19] used hexamethyldisilazane and n-butanol as surface modifiers to prepare SiO_2-Al_2O_3 composite aerogels with specific surface areas of 114 m²·g^{-1} and 183 m²·g^{-1}, respectively; Pu et al.[20] used fly ash to prepare SiO_2-Al_2O_3 composite aerogel with a small specific surface area of only 44.47 m²·g^{-1}.

The removal of CO_2 by potassium-based adsorbent is related to the active components. The above research focuses on the preparation of carrier, the large gap in the structure of gel, the large error in taking the decomposition rate as the index, and the carbonation reaction of K_2CO_3 supported by SiO_2-Al_2O_3 composite aerogel is relatively few, and the mechanism explanation is insufficient. Based on

this, this paper aims to use fly ash to prepare SiO_2-Al_2O_3 composite aerogel and K_2CO_3 loading modification, which integrates preparation and loading and is used as CO_2 adsorbent. We study the CO_2 adsorption performance under different loading rates, explore the decarburization characteristics and cycle mechanism of adsorbent, and provide a theoretical basis for decarburization in the future.

2. Experimental section

2.1 Adsorbent preparation

The flow chart of adsorbent preparation is shown in **Figure 1**. The specific preparation process is as follows: (1) mix fly ash and Na_2CO_3 in proportion and put it into muffle furnace, temperature programmed and calcined; (2) pour a certain con-centration of hydrochloric acid into the calcined product, react with a magnetic stirrer at 40 °C for 50 minutes, and centrifuge the supernatant; (3) drop ammonia water glass rod, stir for 5 minutes, seal and stand at room temperature, seal with ethanol layer after gel, age in water bath at 50 °C for 24 hours to form alcohol gel, and replace the ethanol layer every 8 hours; (4) mix and dissolve K_2CO_3 (0%, 10%, 20%, 25%, 30%, 40%) with alcohol gel in an appropriate amount of deionized water, stir with a magnetic stirrer at room temperature for 12 hours and fully soak; (5) the mixture is put into 100 °C oven for 12 hours to remove the free water in the sample, and then roasted in 300 °C muffle furnace for 2 hours to complete the preparation.
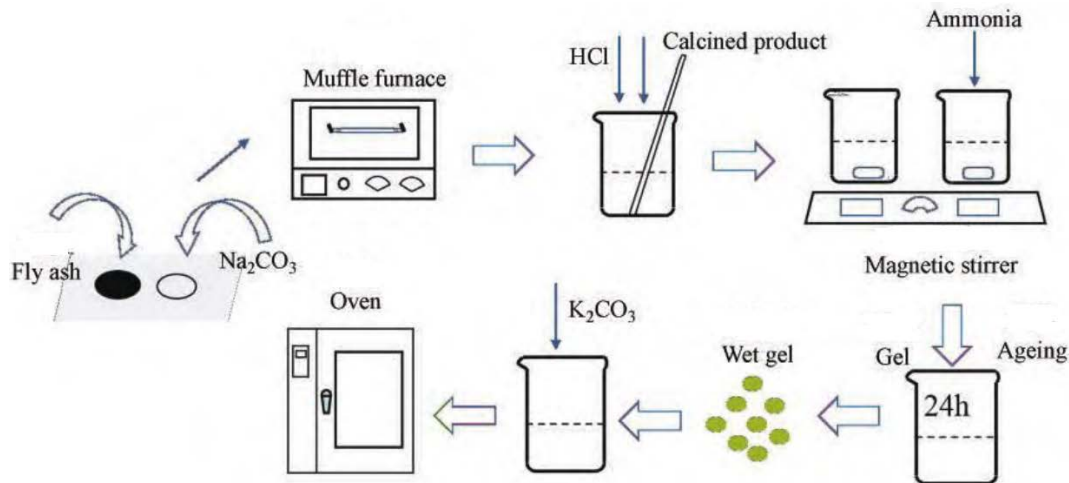
Figure 1. Preparation flow chart of adsorbent.

2.2 Carbonation test system

Generally, the flue gas of coal-fired power station boiler consists of 10%–15% CO_2, 8%–17% steam, a small amount of O_2, a trace of SO_2 and NO_X and most N_2[21]. To simulate the actual flue gas environment, the volume concentration of CO_2 and steam at the inlet is set at 10%, the concentration of N_2 is set at 80%, and the total gas volume is 500 ml·min^{-1}. The test system is shown in **Figure 2**. CO_2 and N_2 are provided by steel cylinders, and the opening is controlled by a mass flow meter. The water vapor is produced by the Series III metering water pump through electric heating and vaporization, and it is mixed with CO_2 and N_2 into the gas mixing tank. When the CO_2 concentration at the outlet and the inlet are the same, the reaction is over, and the experimental data is recorded and effective calculation is performed.

The cumulative adsorption capacity q (mmol·g^{-1}) and CO_2 penetration rate η (%) of unit mass adsorbent are adopted study the decarburization characteristics of adsorbent, and calculate them respectively through equations (1) and (2) (according to standard working conditions):

$$q = T_0/T \, (1000/mV_m) \int_0^t Q(C_1 - C_2/1 - C_2)\mathrm{d}t$$

(1)

$$\eta = \frac{C_1}{C_2} \times 100\%$$

(2)

Where, C_1 and C_2 are the CO_2 concentration at the inlet and outlet, %; Q is the simulated flue gas flow, mL·min^{-1}; t is the reaction time, min; m is the

mass of fixed bed potassium-based adsorbent, g; T is the reaction temperature, K; T_0 is absolute zero

273 K; V_m is the molar volume of gas under standard conditions, 22.4 mol·L^{-1}.
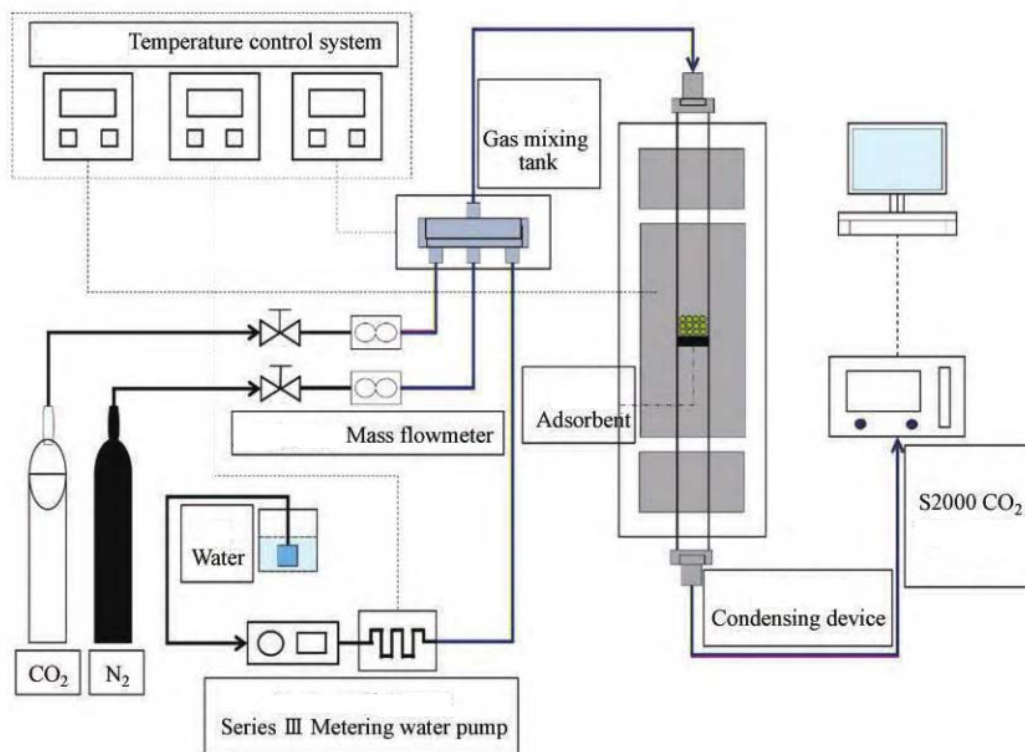
Figure 2. Carbonation reaction system.

Table 2 Chemical composition of fly ash from pulverized coal furnace

Main ingredients	Quality score/%
SiO$_2$	50.26
Al$_2$O$_3$	35.88
Fe$_2$O$_3$	6.00
CaO	2.43
TiO$_2$	1.54
K$_2$O	1.35
SO$_3$	1.11
other	1.43

2.3 Characterization

In this paper, Tescan Mira3 field emission scanning electron microscope was used for SEM test, and the surface micro morphology of the adsorbent was obtained; N$_2$ adsorption desorption test was carried out on potassium-based adsorbent by N$_2$ adsorption desorption instrument, and the adsorption desorption isotherm was obtained to explore the pore structure characteristics of adsorbent. Through BET equation and BJH algorithm, the specific surface area, specific pore volume and other related pore structure parameters of each sample are analyzed; the chemical composition was obtained by all element scanning and conversion calculation with the Netherlands E3 XRF tester; the crystal structure was analyzed by DX2700B XRD tester.

3. Results and discussion

3.1 Selection of preparation conditions of SiO$_2$-Al$_2$O$_3$ composite aerogel

The chemical composition of pulverized coal boiler fly ash obtained by XRF tester is shown in **Table 2**. The main components are SiO$_2$ and Al$_2$O$_3$, with a mass fraction of 86%. It also contains a small amount of iron, calcium, titanium, potassium, sulfur and other impurities. The silicon aluminum content is huge, which can be used as a good raw material for silicon aluminum aerogel.

Silicon and aluminum are mainly composed of mullite (Al$_6$Si$_2$O$_{13}$) and quartz (SiO$_2$) in fly ash. Due to the low reaction activity of mineral crystals, in order to fully extract the silicon and aluminum components, it is necessary to carry out alkali fusion sintering activation treatment on the fly ash under high temperature conditions, and convert the

acid insoluble mullite based phase and alkali (Na_2CO_3) in the fly ash into acid soluble nepheline ($KNa_3[AlSiO_4]_4$) based phase[20] through high temperature sintering reaction, so as to improve the reaction activity and separate the silicon and aluminum components.

Alkali fusion sintering activation[19] is the key to the preparation of SiO_2-Al_2O_3 composite aerogel from fly ash. Generally, the main factors affecting the activation reaction of alkali fusion sintering are: reaction temperature, reaction time and alkali addition ratio. In order to determine the best calcination system and prepare SiO_2-Al_2O_3 composite aerogel with rich pore structure, the specific surface area of SiO_2-Al_2O_3 composite aerogel is selected as the index to measure the activation effect, and the orthogonal test L_9 (3^3) with three factors and three levels is designed, as shown in **Table 3** and **Table 4**.

Table 3. Factor level table

Level	Factor		
	Temperature reflux/°C	Reaction time/min	Alkali addition ratio/(*m* ash: *m* sodium carbonate)
1	800	60	0.5
2	850	90	0.6
3	900	120	0.7

Table 4. Orthogonal test L9(3^3) and range analysis

Test No.	Factor			Specific surface area/(m²·g⁻¹)
	Temperature reflux/°C	Reaction time	Alkali addition ratio/(*m* ash:*m* sodium carbonate)	
1	800	60	0.5	274
2	800	90	0.6	143
3	800	120	0.7	202
4	850	60	0.6	219
5	850	90	0.7	215
6	850	120	0.5	231
7	900	60	0.7	239
8	900	90	0.5	209
9	900	120	0.6	276
K_1	206	244	238	—
K_2	222	189	213	—
K_3	241	236	219	—
R	35	55	25	—

K_i in **Table 4** is the average value of the sum of the indicators of each factor level. The greater the K_i value, the greater the impact of a certain level on the test indicators. R is the extreme difference, and R is the maximum, which means that this parameter has the greatest impact on the test index within the test range. The range analysis results show that the primary and secondary effects of various factors affecting the activation of alkali fusion sintering are: reaction time > reaction temperature > alkali addition ratio. Considering the primary and secondary effects of various factors, the influence of energy consumption and the range results, the optimal combination of reaction conditions in this test is: 900 °C, reaction for 60 minutes, Na_2CO_3 addition ratio of 0.5.
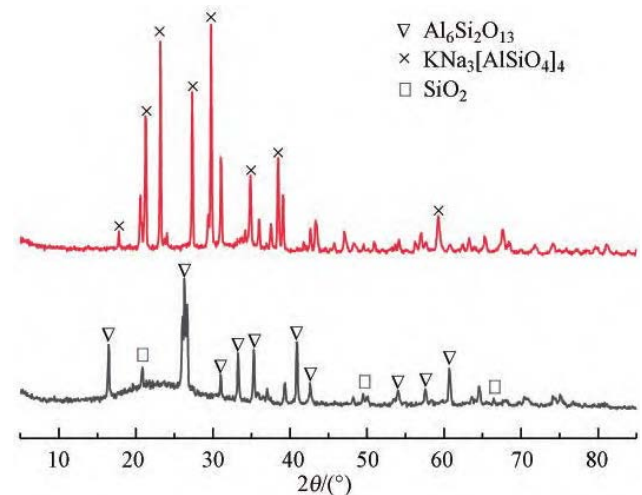
Figure 3. XRD diffraction pattern.
Note: The upper figure represents the products of fly ash and alkali calcination; the following figure represents the XRD of fly ash.

Comparing the crystal phase structure of calcined products and fly ash, the phase analysis re-

81

sults are shown in **Figure 3**. The main phase components in fly ash are mullite ($Al_6Si_2O_{13}$) and SiO_2. After alkali fusion sintering activation, the corresponding diffraction peak positions of $Al_6Si_2O_{13}$ and SiO_2 weaken or even disappear, and the corresponding diffraction peak positions of nepheline ($KNa_3[AlSiO_4]_4$) are analyzed obviously. It shows that in the process of Na_2CO_3 activation reaction at high temperature, the internal bonds of Si-O-Si and Si-O-Al are broken, and the crystal phase structure is destroyed[19]. The covalent bond of mullite is transformed into the ionic bond of nepheline, and the inert aluminum silicon component is fully activated to form a $KNa_3[AlSiO_4]_4$ frame structure evenly distributed in three-dimensional space[21], which provides a theoretical basis for the preparation of SiO_2-Al_2O_3 composite aerogel.

3.2 Carbonation characteristics of supported adsorbents

In this experiment, the SiO_2-Al_2O_3 composite aerogel prepared by loading K_2CO_3 to the best calcination system is made into a loaded adsorbent to improve the capture rate of potassium CO_2. At the same time, the carbonation characteristics of the modified potassium-based adsorbent under different loading conditions were studied, and the adsorption mechanism of the adsorbent was studied combined with the apparent morphology and microscopic characteristics.

(1) Load performance. The carbonation test was carried out under the atmosphere of 60 ℃, $10\%CO_2 + 10\%H_2O + 80\%N_2$ to study the co capture performance of potassium-based adsorbent at 10%, 20%, 25%, 30% and 40% load. The results are shown in **Figures 4** and **Figure 5**.

The adsorption capacity of SiO_2-Al_2O_3 composite aerogel carrier for CO_2 is the lowest, only 0.68 mmol·g^{-1}; in the range of 10%–40%, the CO_2 adsorption capacity of the loaded adsorbent increases first and then decreases with the increase of the proportion of the loaded components. When the loading capacity is 30%, it reaches the maximum, which is 2.86 mmol·g^{-1}. The carbonation performance is excellent, indicating that the CO_2 adsorption is mainly achieved through the chemical reac-

tion of K_2CO_3.
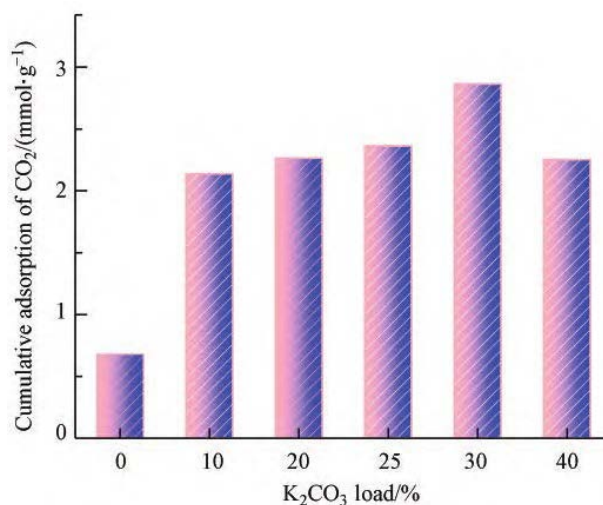
Figure 4. Cumulative adsorption capacity of adsorbent with different loading.
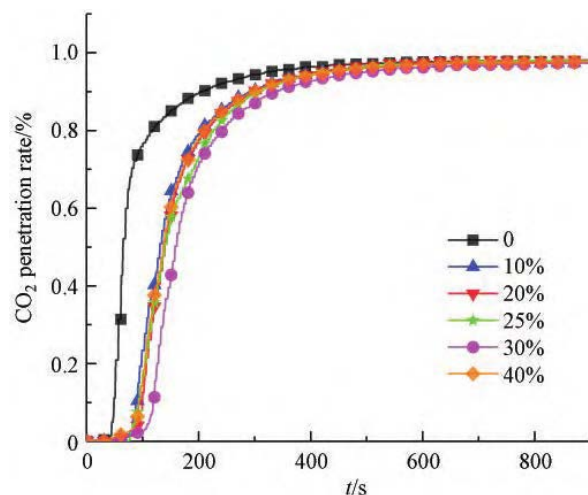
Figure 5. CO_2 breakthrough curves of different loading adsorbents.

When the loading increased from 10% to 30%, the active component K_2CO_3 gradually increased, promoting the reaction to the positive direction when the active component increases to a certain extent, the CO_2 adsorption capacity decreases, which is because the distribution of K_2CO_3 on the carrier surface has reached a saturated state. The more K_2CO_3 is loaded, the K_2CO_3 active sites that can be attached to the carrier surface have been occupied, and the contact between the active component and the gas has reached saturation[22]. At the same time, excessive K_2CO_3 load will plug the pore structure, destroy the CO_2 diffusion process, and reduce the diffusion and utilization efficiency of

82

K_2CO_3. Secondly, during the carbonation reaction, $KHCO_3$ is generated on the surface of the carrier[23], which is not conducive to the reaction.

Under the same test conditions, the higher the η value at the same time, the worse the decarburization performance of the corresponding adsorbent sample. Observe the CO_2 breakthrough curves of the adsorbents with different loadings. At the same time, the η value is the lowest at 30% loading, and the adsorbent CO_2 permeation time is the longest and the adsorption effect is the best, which is consistent with the cumulative adsorption amount.

(2) Microscopic characteristics. The pore structure parameters that affect the decarburization characteristics of adsorbent mainly include specific surface area, cumulative pore volume, relative specific pore volume, etc.[24] When the loading amount increases from 10% to 40%, the N_2 adsorption amount gradually decreases, and the specific surface area and cumulative pore volume are reduced relative to the pure carrier (as shown in **Table 5**). At the same time, the loading of K_2CO_3 reduces the pore richness of the adsorbent, because K_2CO_3 will attach a large amount to the surface and pores of the carrier during the loading process[25]. At this time, the specific surface area Z per unit volume is introduced to characterize its pore abundance, as shown in formula (3):

$$Z = S_0/V_0$$

(3)

Where, S_0 is the specific surface area of adsorbent BET, $m^2 \cdot g^{-1}$; V_0 is the total specific pore volume of adsorbent, $cm^3 \cdot g^{-1}$.

Table 5. Structure parameters of adsorbent pores with different loadings

K_2CO_3 load/%	BET specific surface area/($m^2 \cdot g^{-1}$)	Cumulative pore volume/($cm^3 \cdot g^{-1}$)	Average pore diameter/nm	Pore richness Z	Relative pore volume/%		
					Microporous	Mesoporous	Big hole
10	153.9782	0.3639	8.4944	423.1600	0.2130	93.0500	6.7370
20	110.7819	0.2749	8.9543	402.9385	0.3338	94.2127	5.4536
25	96.6573	0.2695	9.9113	358.6302	0.0988	92.7080	7.1932
30	90.4104	0.2626	11.2873	344.2894	0.0282	90.8132	9.1586
40	85.2602	0.2254	9.5784	378.2618	0.1780	89.3174	10.5027

Low temperature N_2 adsorption desorption tests were carried out on adsorbent samples under different loading conditions to explore the pore structure characteristics of adsorbents. At the same time, the adsorption desorption isotherms and pore size distribution curves of each sample were analyzed. The results are as follows.

Observe the adsorption and desorption isotherms of SiO_2-Al_2O_3 composite aerogel and adsorbent (see **Figure 6**). According to the classification of IUPAC (International Union of Pure and Applied Chemistry), it belongs to type IV isotherm[26], which shows that it is an ordered mesoporous material with relatively uniform pore size distribution, which is conducive to the diffusion and adsorption of gas CO_2 in the pores, and the adsorption and desorption isotherms of adsorbent have not changed significantly after loading, indicating that the loading has little effect on the pore structure of aerogel gel.
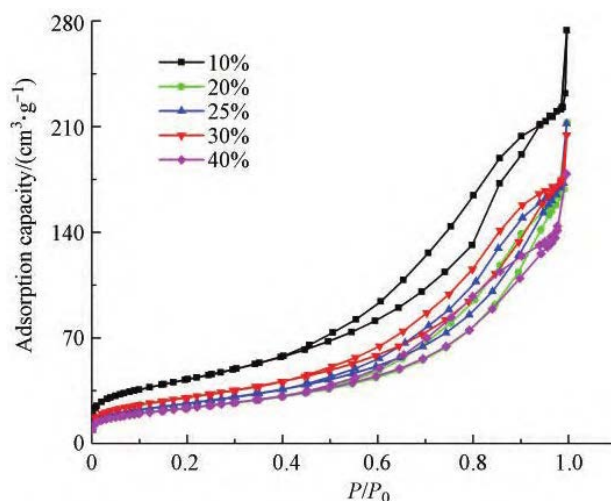
Figure 6. Absorption and desorption isotherms of adsorbents with different loadings.
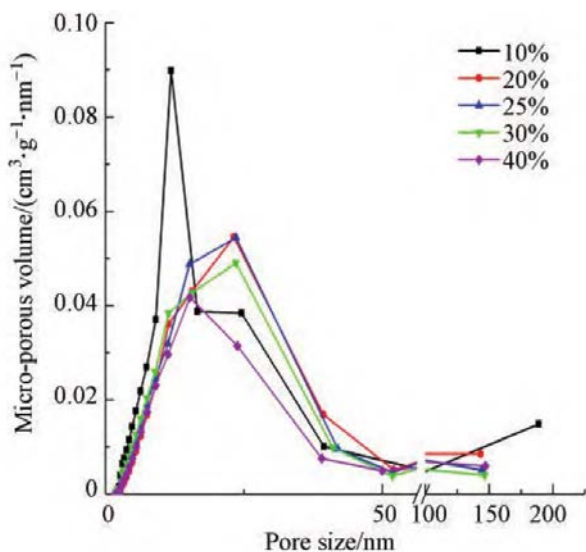
Figure 7. Pore size distribution curve of adsorbent with different loading.

Figure 7 shows the pore size distribution curve of the adsorbent under different loads. The pore size is evenly distributed between 3–50 nm, mainly composed of mesopores and a small number of macropores. On the one hand, adsorbents with larger specific surface area and specific pore volume can provide more active sites; on the other hand, it makes the distribution of the active component K_2CO_3 more uniform, which is conducive to the contact between CO_2 molecules and K_2CO_3 and promotes the carbonation reaction[27]. The peak value in the aperture distribution curve represents the hole with the widest aperture distribution. With the increase of load, the peak value first shifts to the right and then to the left, and the hole volume decreases significantly. When the loading amount increased from 10% to 40%, the pore volume percentage of mesopores decreased from 94.21% to 89.32%, and the pore volume percentage of macropores increased from 5.45% to 10.50%, indicating that the active component K_2CO_3 was mainly filled in the mesopores. The average pore diameter is the ratio of the cumulative total pore internal surface area to the cumulative pore volume. With the decrease of the relative specific pore volume of mesopores, the relative specific pore volume of macropores increases, which makes the average pore diameter increase.
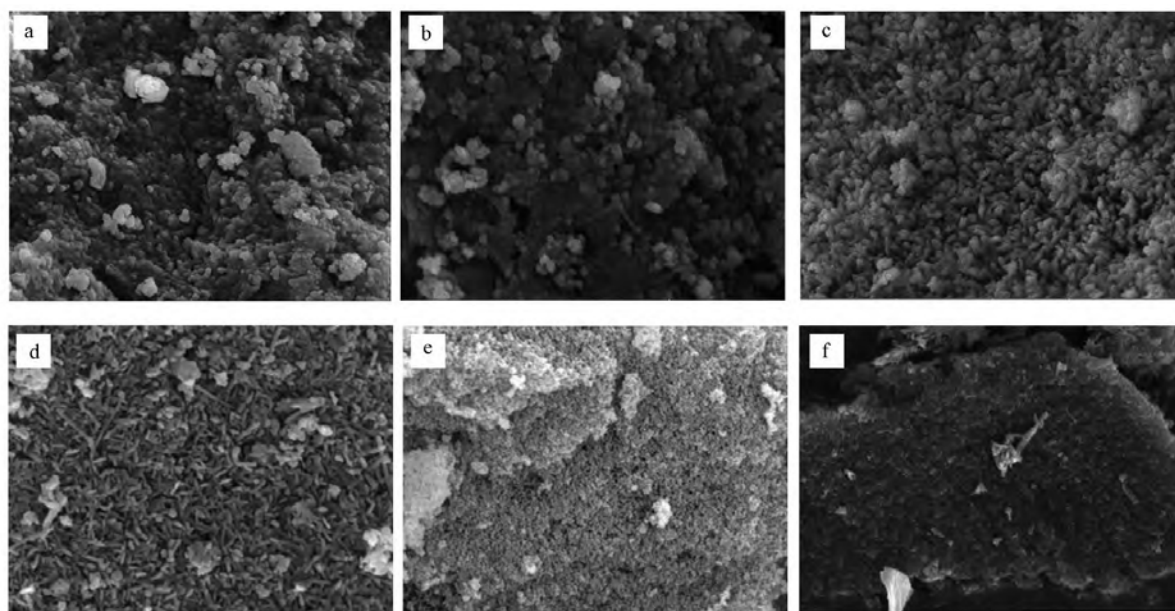
Figure 8. SEM particle morphology of different loading adsorbents (×5,000).

(3) Apparent morphology. **Figure 8** shows the SEM particle morphology distribution of adsorbents with different K_2CO_3 loading. It is found that the surface of SiO_2-Al_2O_3 composite aerogel gel carrier (**Figure 8a**) is loose and has rich pore structure. When the loading amount of K_2CO_3 increases from 10% (**Figure 8b**) to 20% (**Figure 8c**), the porosity of particles begins to decrease; K_2CO_3 mainly fills the interstices between particles and a part of mesopores, and K_2CO_3 crystals are distributed on the

84

surface of the carrier as small white particles. When the loading amount of K_2CO_3 continues to increase from 25% (**Figure 8d**) to 30% (**Figure 8e**), the surface of the adsorbent is stacked by small particles and begins to become more dense, indicating that the loading changes the apparent morphology of the carrier, makes the distribution of K_2CO_3 more uniform, and is conducive to the diffusion of gas to the solid surface, which is consistent with the conclusions of Chen *et al.*[11]. In addition, there are white crystalline substances on the surface of the carrier[28], which may be caused by the introduction of a large number of chloride ions during the preparation process. The crystalline substances are salt compounds composed of chloride ions and other metal ions (such as $FeCl_3$, KCl).

Observe the adsorbent surface with a load of 40% (**Figure 8f**). Excessive K_2CO_3 loading blocks the pore structure and destroys the CO_2 diffusion process. After most of the pores on the surface of the carrier are filled and covered, K_2CO_3 crystals begin to appear large agglomerations with less porous structures. When the loading amount is 30%, the particle distribution of potassium-based adsorbent is more uniform and the morphology is better.

3.3 Cyclic decarburization characteristics of loaded adsorbent

The characteristic of cyclic decarburization is an important index to measure whether potassium-based adsorbents can be widely used in practice. In this paper, the adsorbent prepared above is tested for 10 adsorption regeneration cycles, with a total gas volume of 500 mL·min^{-1}. Under the conditions of adsorption temperature of 60 °C, adsorption atmosphere of $80\%N_2 + 10\%H_2O + 10\%CO_2$, regen-

eration temperature of 120 °C, and regeneration atmosphere of pure nitrogen, the cumulative CO_2 adsorption capacity of the adsorbent changes with the number of cycles, as shown in **Figure 9**.
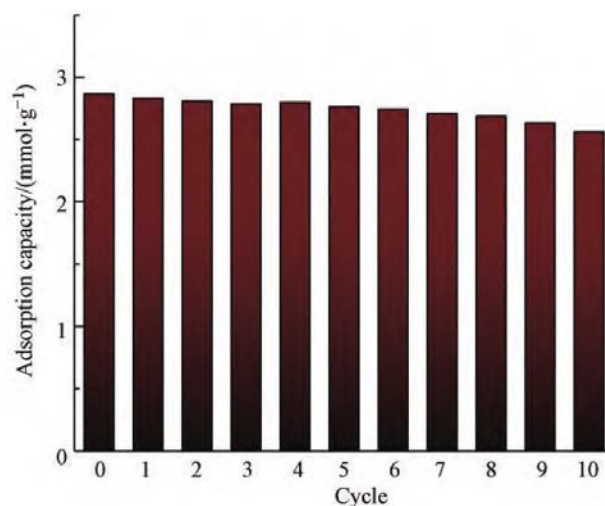
Figure 9. Variation curve of circulating adsorption amount of potassium-based adsorbent.

It can be seen from **Figure 9** that the cumulative adsorption capacity of adsorbent decreases gradually with the increase of adsorption and desorption cycles. After 10 adsorption regeneration cycles, the CO_2 adsorption capacity decreases from 2.86 mmol·g^{-1} to 2.56 mmol·g^{-1}, which still has a good adsorption effect, and the regeneration rate of adsorbent can reach 89.51%. The pore structure analysis of the samples after 10 cycles of regeneration is shown in **Table 6**. It is found that the specific surface area and specific pore volume have little change, indicating that the structure of the prepared adsorbent is stable and the cyclic decarburization performance is good.

Table 6. Changes of potassium-based adsorbent circulation structure parameters

	BET specific surface/(m²·g⁻¹)	Cumulative pore volume/(cm³·g⁻¹)	Most probable aperture/nm	Pore richness Z
30% loaded adsorbent	90.4104	0.2626	11.2873	321.3945
After 10 cycles of regeneration	85.3012	0.2263	9.7932	368.5217

4. Conclusion

(1) Using fly ash as raw material, SiO_2-Al_2O_3 composite aerogel with good pore structure was prepared by sol-gel method. Taking the specific

surface area of SiO_2-Al_2O_3 composite aerogel as the measurement index, the optimal calcination system for alkali fusion sintering activation is determined with orthogonal test: 900 °C, reaction for 60

minutes, Na_2CO_3 addition ratio of 0.5.

(2) The loading amount of K_2CO_3 increased from 10% to 40%, and the specific surface area and cumulative pore volume decreased. The cumulative adsorption amount of CO_2 increased first and then decreased. When the loading amount was 30%, the maximum cumulative adsorption amount of CO_2 was 2.86 mmol·g^{-1}, which was consistent with the result of CO_2 penetration rate.

(3) The more the loading amount is, the K_2CO_3 active site that can be attached to the surface of the carrier has been occupied, and the contact between the active component and the gas has reached saturation. Excessive K_2CO_3 load will plug the pore structure, destroy CO_2 diffusion, and reduce diffusion and utilization efficiency. During the reaction, $KHCO_3$ is formed on the surface of the carrier, which is not conducive to the reaction.

(4) The pore volume percentage of mesopores decreased from 94.21% to 89.32%, indicating that the active component K_2CO_3 was mainly filled in the mesopores. On the one hand, adsorbents with larger specific surface area and specific pore volume can provide more active sites. On the other hand, it makes the distribution of active component K_2CO_3 more uniform, which is conducive to the diffusion of gas to the solid surface and promotes the carbonation reaction.

(5) After 10 adsorption regeneration cycle tests, the CO_2 adsorption capacity of the adsorbent decreased by 10.49%. At the same time, the microstructure parameters of the adsorbent did not change greatly, the structure was stable, and the cycle decarburization performance was good.

Acknowledgements

Conflict of interest

The authors declare no conflict of interest.

References

1. Sun Q. Analysis of the current situation of China's carbon emission market construction. Value Engineering 2019; 38(26): 120–121.

2. Zhang T, Ma W, Qi X, *et al*. Characteristics and sources of organic carbon and element carbon in PM2.5 in the urban areas of Beijing. Environmental Chemistry 2018; 37(12): 2758–2766.

3. Zhao C, Chen X, Zhao C. Research progress of CO_2 capture technology using dry alkali-based sorbents. Journal of Power Engineering 2008; 28(6): 827–833.

4. Cui S, Cheng W, Shen XD. Mesoporous amine-modified SiO_2 aerogel: A potential CO sorbent. Energy & Environmental Science 2011; 4(6): 2070–2074.

5. Dong W, Chen X, Yu F, *et al*. Carbonation characteristics of sodium-based solid sorbents for CO_2 capture. Journal of China Coal Society 2015; 40(9): 2200–2206.

6. Liang C. Study on CO_2 capture performance of biomass-templated CaO-based sorbent pellets [MSc thesis]. Nanjing: Nanjing Normal University; 2019.

7. Yang F, Fu J, Zou C, *et al*. Synthesis of $MgCl_2$ modified carbon materials for CO_2 adsorption. Environmental Chemistry 2019; 38(11): 2555–2562.

8. Lee SC, Kim JC. Dry potassium-based sorbents for CO_2 capture. Catalysis Surveys from Asia 2007; 11(4): 171–185.

9. Lee SC, Choi BY, Lee TJ, *et al*. CO_2 absorption and regeneration of alkali metal-based solid sorbents. Catal Today 2006; 111(3): 385–390.

10. Zhao CW, Guo YF, Li CH, *et al*. Remove of low concentration CO_2 at ambient temperature using several potassium-based sorbents. Applied Energy 2014; 124(7): 241–247.

11. Zhao C. Investigations on CO_2 capture characteristics of dry potassium-based sorbent (in Chinese) [PhD thesis]. Nanjing: Southeast University; 2011.

12. Lee SC, Chae HJ, Lee SJ, *et al*. Novel regenerable potassium-based dry sorbents for CO_2 capture at low temperatures. Journal of Molecular Catalysis B: Enzymatic 2009; 56(2): 179–184.

13. Liu Y, Xu L, Song K, *et al*. Carbonation characteristics of supported K_2CO_3/5A adsorbent. Chemical Engineering 2018; 46(7): 12–16.

14. Guo YF, Zhao CW, Sun J. Facile synthesis of silica aerogel supported K_2CO_3 sorbents with enhanced CO_2 capture capacity for ultra-dilute flue gas treatment. Fuel 2018; 215(3): 735–743.

15. Chen S, Zhao C, Zhao C. Development of CO_2 capture technology using solid potassium-based sorbents. Journal of Power Engineering 2010; 30(7): 542–549.

16. Feng J, Gao Q, Wu W, *et al*. Effect of silica content on structure and properties of Al_2O_3-SiO_2 aerogels. Chinese Journal of Inorganic Chemistry 2009; 25(10): 1758–1763.

17. Yu Y, Ma R, Wang G, *et al*. Preparation and characterization of Al_2O_3 bulk aerogel with high specific surface area and low density. Journal of Materials Engineering 2019; 47(12): 136–142.

18. Liu B, Liu M, Chen X. Preparation of SiO_2-Al_2O_3 composite aerogel with high specific surface area by sol-gel method from coal gangue. CIESC Journal

2017; 68(5): 2096–2104.

19. Chen N, Yan Y, Hu Z, *et al*. Research of SiO_2-Al_2O_3 aerogel with fly ash. Journal of Wuhan University of Technology 2011; 33(2): 37–41.

20. Pu K, Chen N, Li B. Study on the preparation of silicon-aluminum aerogel from fly ash (in Chinese). Development Guide to Building Materials 2017; 15(18): 1672–1675.

21. Xu Z. Study on the preparation & modification and pelletization of sodium-based CO_2 solid sorbents [MSc thesis]. Nanjing: Southeast University; 2019.

22. Guo BH, Wang YL, Guo JN, *et al*. Experiment and kinetic model study on modified potassium-based CO_2 adsorbent. Chemical Engineering Journal 2020; 399: 125849.

23. Amiri M, Shahhosseini S. Optimization of CO_2 capture from simulated flue gas using K_2CO_3/Al_2O_3 in a micro fluidized bed reactor. Energy and Fuels 2018; 32(7): 7978–7990.

24. Kong Y, Shen XD, Cui S, *et al*. Development of monolithic adsorbent via polymeric sol-gel process for low-concentration CO_2 capture. Applied Energy 2015; 147: 308–317.

25. Linneen N, Pfeffer R, Lin YS. CO_2 capture using particulate silica aerogel immobilized with tetra-ethylenepentamine. Microporous and Mesoporous Materials 2013; 176: 123–131.

26. He Y, Li Z, Xi H. Research progress of gas-solid adsorption isotherms. Ion Exchange and Adsorption 2014; 20(4): 276–289.

27. Kong Y, Jiang GD, Fan MH, *et al*. A new aero-gel-based CO_2 adsorbent developed using a simple sol-gel method along with supercritical drying. Chemical Communication 2014; 50(81): 12158–12161.

28. Huang YQ, Liu HC, Yuan HY, *et al*. Migration and speciation transformation of K and Cl caused by interaction of KCl with organics during devolati-lization of KCl-loaded model biomass compounds. Fuel 2020; 277: 118205–118215.

87